Parasitology International 68 (2019) 40–47

Contents lists available at ScienceDirect

Parasitology International

journal homepage: www.elsevier.com/locate/parint

Infection dynamics of *Toxoplasma gondii* in gut-associated tissues after oral infection: The role of Peyer's patches☆

Tetsuya Mitsunaga[a,b,*], Kazumi Norose[a,*], Fumie Aosai[a,c], Hiroshi Horie[d], Naomi Ohnuma[b], Akihiko Yano[a]

[a] Department of Infection & Host Defense, Graduate School of Medicine, Chiba University, 1-8-1 Inohana, Chuo-ku, Chiba 260-8670, Japan
[b] Department of Pediatric Surgery, Graduate School of Medicine, Chiba University, 1-8-1 Inohana, Chuo-ku, Chiba 260-8670, Japan
[c] Department of Infection and Host Defense, Graduate School of Medicine, Shinshu University, 3-1-1 Asahi, Matsumoto 390-8621, Japan
[d] Department of Pathology, Chiba Children's Hospital, 579-1 Heta-cho, Midori-ku, Chiba 266-0007, Japan

ARTICLE INFO

Keywords:
Toxoplasma gondii
Peyer's patches
Ileum
Mesenteric lymph node
Interferon gamma (IFN-γ)

ABSTRACT

Toxoplasma gondii is a common perorally transmitted parasite; however, its immunopathogenesis in gut-associated tissues remains unclear. Here, we compared disease manifestation in C57BL/6 immunocompetent wild type (WT) mice and immunocompromised interferon (IFN)-γ-deficient (GKO) mice after peroral infection (PI) with *T. gondii* cysts (Fukaya strain). Strong PI-induced Th1 cytokine expression was detected in WT mice. Moreover, bradyzoite-specific *T.g.HSP30/bag1* mRNA was detected in the ileum parenchyma and Peyer's patches (PP), but not in the mesenteric lymph nodes, at 7 days post-infection in WT mice, and was significantly higher than that in GKO mice. Nested PCR showed that parasites existed in ileum parenchyma at days 1 and 1.5 post-PI in GKO and WT mice, respectively. In addition, quantitative competitive-PCR indicated that *T. gondii* first colonized the PP (day 3 post-PI), followed by the ileum parenchyma and mesenteric lymph nodes, spleen, and portal and aortic blood (day 7 post-PI). Although parasites were consistently more abundant in GKO mice, similar invasion and dissemination patterns were observed in the two hosts. Collectively, these data suggest that some zoites differentiate from tachyzoites to bradyzoites in the ileum and that *T. gondii* initially invades the ileum parenchyma, and then accumulates and proliferates in the PP before disseminating through the lymphatic systems of both GKO and WT hosts.

1. Introduction

The obligate intracellular protozoan parasite *Toxoplasma gondii* is a food- and water-borne pathogen that can cause disease in humans and animals. *T. gondii* generally invades the host through the lining of the intestine after peroral infection (PI) by bradyzoites or oocysts [1], which can lead to lethal ileitis [2] and colitis [3]. The gut mucosal immune system serves as the frontline of defense against this parasite [4]. Following antigenic stimulation, the mucosa-associated lymphoid tissues (MALTs) can induce an immune response characterized by lymphocyte proliferation and differentiation. These lymphocytes then egress from the secondary lymphoid tissues into the bloodstream [5,6]. Although Peyer's patches (PPs) are MALTs and are thus inductive sites of mucosal immunity [7], the precise roles mediated by the PP in response to peroral *T. gondii* infection remain unclear.

Pathogens employ a variety of mechanisms to escape detection by host defense systems as they disseminate either lymphogenously or hematogenously [8]. Many reports have described the kinetics of parasitic dissemination routes after *T. gondii* PI [1,8–13], which differ based on strain, mouse genotype, and inoculation (oral gavage or natural feeding) and detection methods. In addition, a rigorous analysis of stage conversion in gut-associated tissues has not been performed to date.

Recent studies have revealed that *T. gondii* infection is a significant cause of morbidity and mortality in immunocompromised hosts, such as patients with acquired immunodeficiency syndrome (AIDS) or organ transplant patients treated with immunosuppressive drugs [14,15]. As such, the infection dynamics of *T. gondii* in both immunocompromised and immunocompetent hosts need to be clarified. Control of toxoplasmosis has been extensively studied in mouse models, and it has

☆ Original paper

* Corresponding authors at: Department of Infection & Host Defense, Graduate School of Medicine, Chiba University, 1-8-1 Inohana, Chuo-ku, Chiba 260-8670, Japan.
E-mail addresses: tetsuya@z.email.ne.jp (T. Mitsunaga), norose@faculty.chiba-u.jp (K. Norose).

https://doi.org/10.1016/j.parint.2018.08.010
Received 7 November 2017; Accepted 31 August 2018
Available online 03 September 2018
1383-5769/

been demonstrated that interferon (IFN)-γ responses are critical for protection against this parasite [16,17]. As *IFN*-γ gene-deficient (GKO) mice are unable to resist *T. gondii* infection, they can therefore be considered as a representative model of immunocompromised hosts for *T. gondii* infection.

In this study, we have performed the cytokine levels, stage-conversion status (tachyzoites vs. bradyzoites), and histopathology of the digestive tract tissues from C57BL/6 immunocompetent wild type (WT) and immunocompromised GKO mice during acute phase of infection. Furthermore, very early invasion route was assessed by nested polymerase chain reaction (PCR) targeting *B1* gene [18], and dissemination route by quantitative competitive (QC) PCR targeting *SAG1* gene [10].

2. Material and methods

2.1. Parasites

Cysts derived from the avirulent *T. gondii* Fukaya strain (type II genotype) [19] were prepared from B10.A (4R) mice that had been orally infected with five cysts containing the Fukaya strain, 6 weeks previously [10].

2.2. Animals

Eight- to twelve-week-old C57BL/6 WT (SLC, Hamamatsu, Japan) and same background GKO (a gift from Prof. Yoichiro Iwakura, Center for Animal Disease Models, Research Institute for Biomedical Sciences, Tokyo University of Science, Tokyo, Japan) mice were used for our analyses. GKO mice were maintained in our laboratory and genotyped by PCR [20]. Infection status was assessed in mice euthanized by intraperitoneal injection of 2 mg ketamine hydrochloride at 1, 1.5, and 2 days post-PI. To assess infection dynamics, mice were orally infected with 10 *T. gondii* cysts administered using a syringe fitted with a rounded 19-gauge needle and were euthanized at 1, 3, 5, and 7 days after PI. The abdomen was incised and the peritoneal lining was opened to expose the intestines. The portal vein was ligated at the porta hepatica, and portal blood was collected using a 24-gauge venous cannula. Aortic blood was collected by cardiopuncture. The distal side of the small intestine was removed and washed with cold phosphate-buffered saline (PBS) before being divided longitudinally. All visible PPs were removed using shaped scissors and the remaining tissues were defined as the ileum parenchyma. The mesenteric lymph node (MLN) and spleen were also extracted.

To assess the survival rate, the mice were orally infected with 5 or 10 *T. gondii* cysts. Survival was monitored daily to assess mortality. Animals were treated according to the guidelines established by the Chiba University Animal Ethics Committee.

2.3. Reverse transcriptase (RT)-PCR

mRNA was purified from the ileum parenchyma, PP, and MLN tissues to assess tissue cytokine mRNA expression at 7 days after PI by RT-PCR as described previously [21]. In brief, GITC buffer (4 M guanidinium thiocyanate, 25 mM sodium citrate, 0.1 M 2-mercaptoethanol, 0.5% N-laurylsarcosine) was added to homogenized tissue samples to promote lysis. RNA was then extracted using water-saturated phenol and chloroform/isoamyl alcohol. The prepared mRNA (1 μg) was reverse transcribed in a 20 μL reaction volume using an RNA PCR kit (Takara, Shiga, Japan) according to the manufacturer's instructions. PCR was performed using 5 μL of the resulting cDNA product. Similarly, the expression of *SAG1* (used as a tachyzoite marker) [22] and *T. gondii* (*T.g.*) *Hsp30/bag1* (used as a bradyzoite marker) mRNA [23] was also investigated by RT-PCR 7 days after PI. Glyceraldehyde 3-phosphate dehydrogenase (*Gapdh*) mRNA expression was used as an internal control. The expression levels of mRNA were calculated using the ratio of the respective densities of their RT-PCR products to that of *Gapdh* mRNA.

2.4. Nested PCR and QC-PCR

Total genomic (g) DNA was isolated from the ileum parenchyma, PP, and MLN and used to assess very early infection status by nested PCR with primers targeting *B1* gene [18]. Parasite load and dissemination were determined by assessing *SAG1* DNA in the ileum parenchyma, PP, MLN, spleen, portal blood, and aortic blood by QC-PCR as described previously [10]. In brief, digestion buffer (100 mM NaCl, 10 mM Tris-Cl, pH 8.0, 25 mM ethylenediaminetetraacetic acid, 0.5% sodium dodecyl sulfate, and 0.1 mg/mL proteinase K) was used to homogenize tissues before digestion at 55 °C in a shaking water bath overnight. DNA was extracted as described previously [10]. Prepared gDNA (1 μg) was co-amplified with a constant concentration of truncated *SAG1* DNA, which competitively binds to oligo primers for WT *SAG1* [10]. The amplified cDNA was electrophoresed on a 1% agarose gel containing ethidium bromide. The WT to competitor ratio for amplified *SAG1* DNA (T/C) was measured using an IPLab Gel densitometer (Signal Analytical Corp., VA, USA). The abundance of *T. gondii* was calculated as described previously [10].

2.5. Primers

The primers used were as follows: *IFN*-γ, forward (5′-TGA ACG CTA CAC ACT GCA TCT TGG-3′), and reverse (5'-CGA CTC CTT TTC CGC TTC CTG AG-3′); IL-12, forward (5'-CGT GCT CAT GGC TGG TGC AAA G-3′), and reverse (5′-GAT GAA GAA GCT GGT GCT G-3′); IL-4, forward (5′-GAA TGT ACC AGG AGC CAT ATC-3′), and reverse (5'-CTC AGT ACT ACG AGT AAT CCA-3′); IL-10, forward (5'-CGG GAA GAC AAT AAC TG-3′), and reverse (5'-CAT TTC CGA TAA GGC TTG G-3′); SAG1, forward (5'-GGC ATA TGT CGG ATC CCC CTC TTG TTG C-3′), and reverse (5'-GGC TCG AGC TCC AGT TTC ACG GTA CAG T-3′); T.g.Hsp30/bag1, forward (5′-GGG AAT TCA TGG CGC CGT CAG CAT C-3′), and reverse (5′-GGG CGG CCG CCT ACT TCA CGC TGA TTT GTT-3′); Gapdh, forward (5'-ACC ACA GTC CAT GCC ATC AC-3′), and reverse (5'-TCC ACC ACC CTG TTG CTG TA-3′). Two PCR primer pairs were used for *B1* gene nested PCR as follows: S1, 5′-TGT TCT GTC CTA TCG CAA CG-3′ and AS1, 5'-ACG GAT GCA GTT CCT TTC TG-3′; S2, 5'-TCT TCC CAG ACG TGG ATT TC-3′ and AS2, 5'-CTC GAC AAT ACG CTG CTT GA-3′ [18].

2.6. Histopathology

The ileum and MLN were harvested from WT and GKO mice euthanized 8 days after PI with 10 cysts and analyzed histopathologically. The extracted ileum was washed twice in PBS to remove the mucus before being cut longitudinally along the side that adhered to the mesentery. Tissues were fixed in 20% buffered formalin and embedded in paraffin. The paraffin embedded ileum was then cut orthogonally to the axis and stained with hematoxylin and eosin (HE). Images were acquired on a microscope (BX41, Olympus, Tokyo, Japan) equipped with a charge-coupled device camera (FX630, Olympus).

2.7. Drugs

Polymyxin B sulfate (Pfizer Japan Inc., Tokyo, Japan) and metronidazole (Shionogi Co., Ltd., Osaka, Japan) were administered separately or concomitantly in drinking water at 250 U/mL and 50 μg/mL, respectively. Metronidazole was initially dissolved in diluted hydrochloric acid to facilitate water absorption before adjusting the pH to 7 with 2 N NaOH.

2.8. Statistical analysis

Differences between groups were determined by the Mann-Whitney

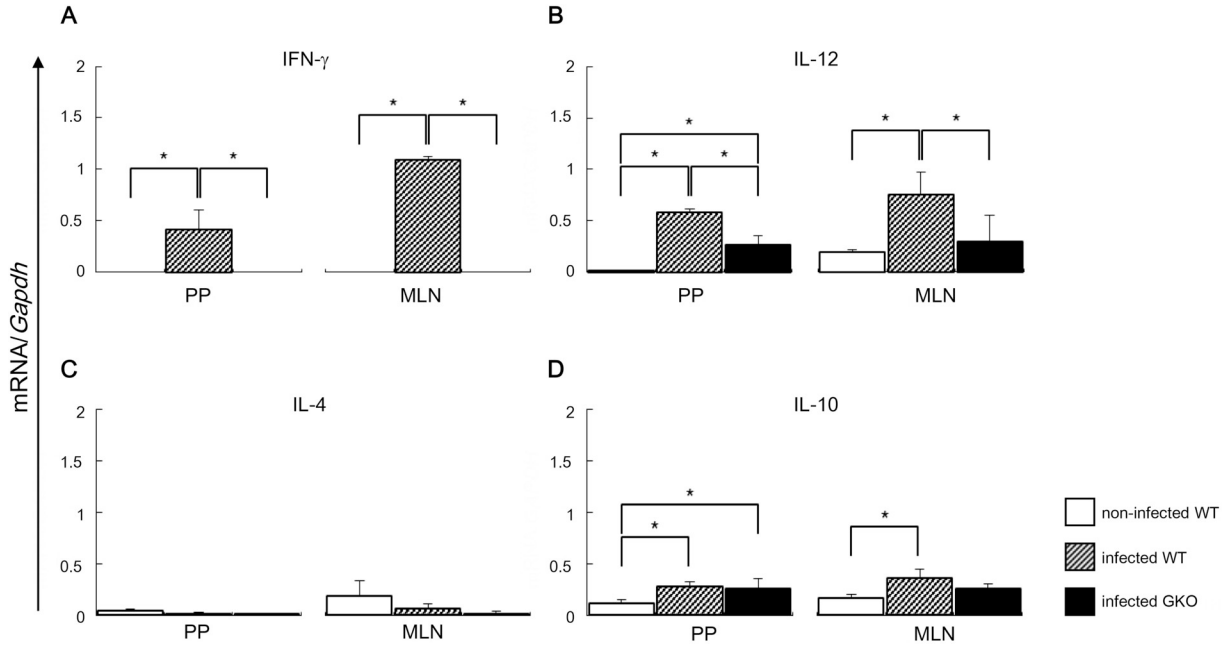

Fig. 1. Comparison of *IFN-γ*, *IL-12*, *IL-4*, and *IL-10* mRNA expression levels in the PP and MLN. C57BL/6 WT mice and GKO mice were perorally inoculated with 10 cysts containing *T. gondii*. The PP and MLN were removed 7 days after PI, and the expression of *IFN-γ*, *IL-12*, *IL-4*, and *IL-10* mRNA per microgram of specimen RNA was investigated by RT-PCR. Non-infected WT mice were used as controls. Results are expressed as the ratio of the optical density (OD) of the RT-PCR product for each molecule and the OD of the *Gapdh* RT-PCR product. Three mice were used in each experimental group and the experiment was repeated twice. Data are presented as mean ± S.D. $^*P < 0.05$.

U test. Survival analysis was performed using the Kaplan-Meier method. $P < 0.05$ was considered statistically significant.

3. Results

3.1. Comparison of cytokine expression in T. gondii-infected WT and GKO mice

We first examined cytokine expression in the PP and MLN of *T. gondii*-infected WT and GKO mice using non-infected WT mice as controls (Fig. 1). As expected, significantly higher levels of *IFN-γ* and *IL-12* mRNA were observed in infected WT mice compared to non-infected controls ($P < 0.05$) (Fig. 1A, B). Although no *IFN-γ* mRNA expression was observed in infected GKO mice, *IL-12* mRNA expression was significantly higher in the PP of infected GKO mice compared to that of the non-infected WT counterparts, but was substantially lower than that in infected WT mice. Conversely, *IL-4* mRNA expression in the PP and MLN tended to decrease in both infected WT and GKO mice as compared to that in non-infected WT controls (Fig. 1C). Moreover, *IL-10* mRNA expression was significantly increased in the PP and MLN of the infected WT mice and in the PP of GKO mice compared to that in non-infected WT mice (Fig. 1D).

3.2. Stage conversion in WT and GKO mice after T. gondii infection

T.g.Hsp30/bag1 (a bradyzoite marker) and *SAG1* (a tachyzoite marker) mRNA expression was investigated to monitor the sites of stage conversion after PI (Fig. 2). In WT mice, increased *T.g.Hsp30/bag1* mRNA levels were observed in the ileum parenchyma and PP 7 days after PI but not in the MLN (Fig. 2A). The *T.g.Hsp30/bag1* bands in the PP were much stronger than those in the ileum parenchyma. By contrast, *SAG1* mRNA expression was detected in all tissues examined (Fig. 2A).

The corresponding stage conversion analysis in GKO mice 7 days after PI revealed detectable *T.g.Hsp30/bag1* mRNA expression in the ileum parenchyma, PP, and MLN (Fig. 2B), although the expression

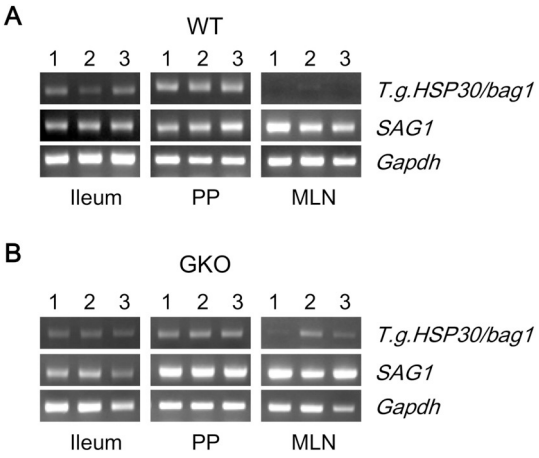

Fig. 2. *T.g.Hsp30/bag1* (a marker of bradyzoites) and *SAG1* (a marker for tachyzoites) mRNA expression in gut-associated tissues. (A) WT and (B) GKO mice were perorally inoculated with 10 cysts containing *T. gondii*. Gut-associated tissues were removed 7 days after PI, and the expression of *T.g.Hsp30/bag1, SAG1*, and *Gapdh* mRNA per microgram of specimen RNA was investigated by RT-PCR. Three mice were used in each experimental group, and the experiment was repeated twice with similar findings observed each time. PP; Peyer's patches, MLN; mesenteric lymph node. The lane number represents the individual mouse from which the samples were obtained.

level was slightly lower in the MLN than in the ileum parenchyma and PP. *SAG1* mRNA was detectable in all GKO mouse tissues with equivalent expression in the PP and MLN (Fig. 2B). Interestingly, *T.g.HSP30/bag1* mRNA expression in the PP of WT mice was significantly higher than that in GKO mice, whereas *SAG1* mRNA expression was higher in the PP and MLN of GKO mice.

3.3. Pathology

Eight days after infection, WT mice developed severe focal

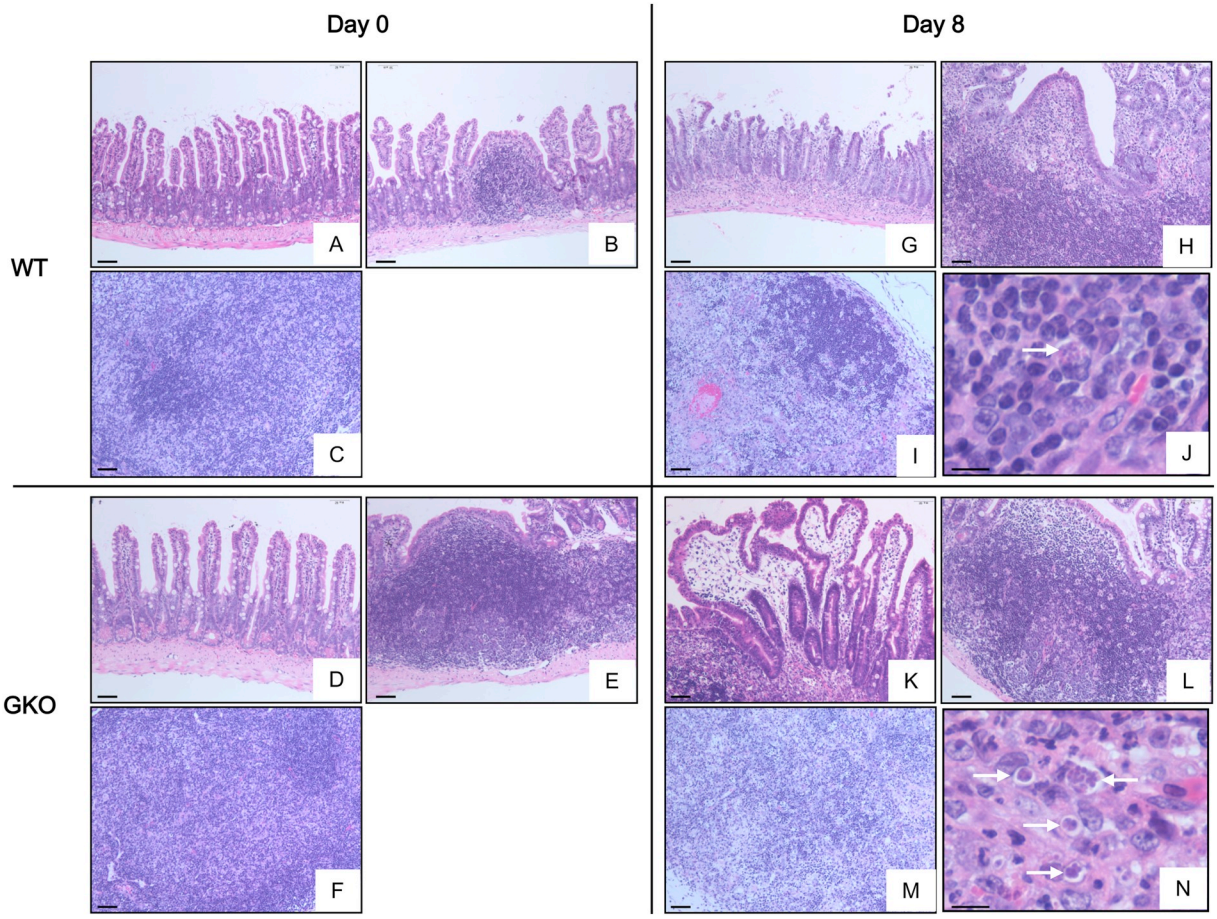

Fig. 3. Inflammation status of the ileum and gut-associated lymphoid tissues 8 days after *T. gondii* PI. Microvilli in WT mice (A and G) and GKO mice (D and K); PP in WT mice (B and H) and GKO mice (E and L); MLN in WT mice (C and I) and GKO mice (F and M). Arrows indicate the presence of *T. gondii* in the PP of WT (J) and GKO mice (N). Scale bars: 50 μm (A–I, K–M) or 10 μm (J, N). Two mice were used in each experimental group, and representative images are shown.

ulcerative and necrotic enteritis, as well as lymphoid follicle inflammation, characterized by a marked increase in inflammatory leukocytes in the ileum, PP, and MLN (Fig. 3G–I). Severe villous edema was much more diffuse in GKO mice than in the WT counterparts (Fig. 3K). In addition, neutrophil infiltration was much more noticeable in the lamina propria than that observed in WT mice. Lymphoid follicle inflammation in the PP and MLN in GKO mice was characterized by the extensive nuclear fragmentation of lymphocytes (Fig. 3L, M), many apoptotic cells in the PP (Fig. 3L), and a disrupted microarchitecture in the MLN (Fig. 3M). High-power views of the ileum harvested from infected WT (Fig. 3J) and GKO (Fig. 3N) mice showed *T. gondii* in the lamina propria (arrows), with much higher parasite numbers seen in the GKO mice.

3.4. Survival rate of WT and GKO mice

Eighty percent of the WT mice survived for > 80 days post-PI with 5 cysts as compared to only 40% of those infected with 10 cysts (Fig. 4A). Conversely, all GKO mice succumbed within 10 days post-PI with 5 or 10 cysts. Significant differences were observed between the survival rates of WT and GKO mice infected with 5 or 10 cysts.

3.5. Influence of enteric bacteria co-infection

The effect of enteric bacteria co-infection on the clinical course and progression of toxoplasmosis was assessed in *T. gondii*-infected GKO mice. Polymyxin B and metronidazole are antibacterial agents used for intestinal sterilization before bone marrow transplantation or digestive surgery [24–26]. Thus, we administered polymyxin B and metronidazole separately or concomitantly to GKO mice starting 3 days before infection, and monitored their survival thereafter. However, all the GKO mice died within 10 days after PI regardless of the treatment combination (Fig. 4B). Moreover, no significant survival difference was found between the untreated and drug-treated groups. In addition, *SAG1* gene was detected in the MLN of all dead mice (data not shown).

3.6. Natural invasion and dissemination route of T. gondii in WT mice

In WT mice, the *B1* gene was first detected in the ileum parenchyma, PP, and MLN at day 1.5 after PI (data not shown). The *SAG1* gene was first found in the PP on day 3, followed by the ileum parenchyma and MLN at day 5, but not in the spleen, portal blood, or aortic blood (Fig. 5A). In addition, *T. gondii* loads in the PP and MLN were significantly higher than those in the portal and aortic blood, ileum parenchyma, and spleen on day 5 ($P < 0.05$). However, protozoa were detectable in the circulatory system by day 7, with increased *T. gondii* loads in the ileum parenchyma, PP, and MLN. Significant differences in *T. gondii* loads were found between the PP and ileum parenchyma, spleen, portal blood, or aortic blood, and in the MLN and ileum parenchyma at day 7 ($P < 0.05$).

3.7. Comparison of parasite load kinetics in WT and GKO mice

B1 gene expression was first observed in the ileum parenchyma at day 1 post-PI in GKO mice, followed by the PP and MLN at day 1.5 after PI (data not shown). In comparison, *SAG1* gene was first detected in the

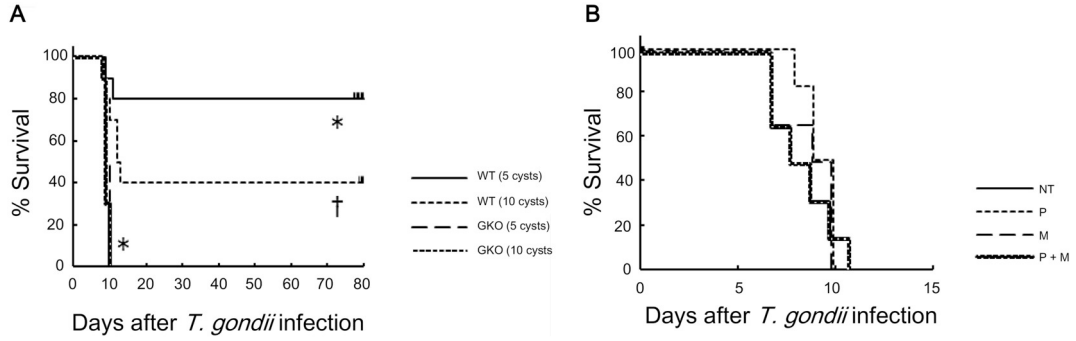

Fig. 4. Survival rate after infection. (A) Comparison of the survival rate of WT and GKO mice after infection perorally with 5 or 10 cysts containing *T. gondii* ($n = 10$ per group). Data are presented using a Kaplan-Meier plot. $^{*}P < 0.05$ compared to GKO mice infected with 5 cysts. $^{\dagger}P < 0.05$, compared to GKO mice infected with 10 cysts. (B) Effects of intestinal sterilization in GKO mice challenged perorally with 10 cysts containing *T. gondii*. Antibiotics were administered to GKO mice from 3 days before infection until death, and survival was monitored daily. NT, no treatment; P, polymyxin B treatment; M, metronidazole treatment; P + M, polymyxin B and metronidazole treatment. Data were analyzed using the Kaplan-Meier method. Six mice were used in each group.

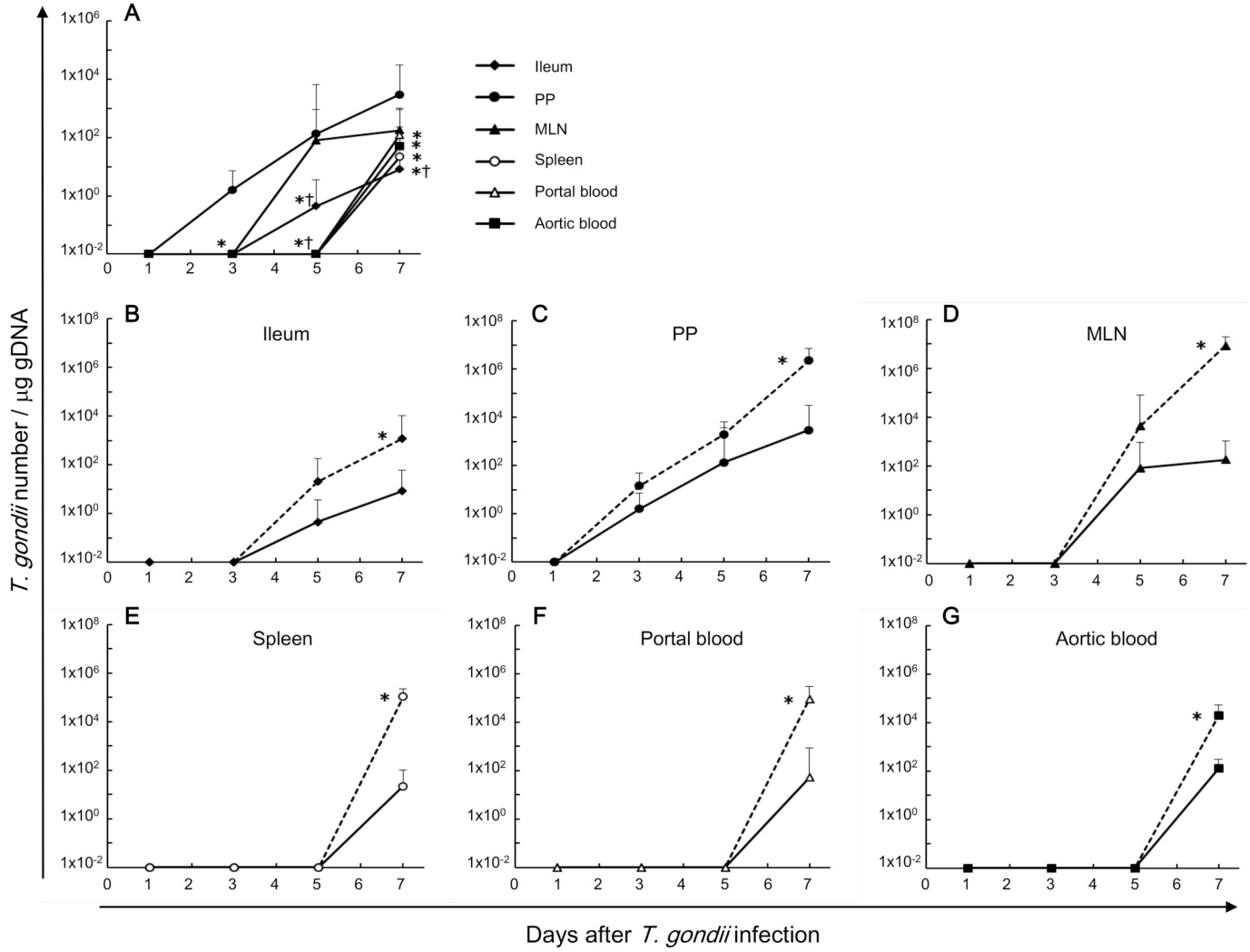

Fig. 5. Parasite load analyzed by QC-PCR. (A) Kinetics of the *T. gondii* load in WT mice following PI as determined by QC-PCR. Results for each tissue and time point were obtained from three mice. Experiments were performed in triplicate, with similar results obtained in each case. Data are expressed as the number of parasites per microgram of specimen DNA, and are presented as the mean ± S.D. Ileum, ileum parenchyma; PP, Peyer's patches; MLN, mesenteric lymph node. $^{*}P < 0.05$ compared to PP. $^{\dagger}P < 0.05$ compared to MLN. (B–G) Kinetics of the *T. gondii* load in WT and GKO mice. Comparison of the number of *T. gondii* in gut-associated tissues at various times after infection of WT (—) and GKO (—) mice: (B) ileum parenchyma, (C) PP, (D) MLN, (E) spleen, (F) portal blood, (G) aortic blood. Data are expressed as the number of parasites per microgram of specimen DNA and are presented as the mean ± S.D. Results were obtained from three mice from each strain. The experiments were performed twice, and similar results were obtained. $^{*}P < 0.05$ compared to WT mice.

PP, followed by detection in the ileum parenchyma and MLN, and finally in the spleen and portal and aortic blood in WT mice (Fig. 5A). Consistently, significantly higher *SAG1* gene expression levels were found in GKO mice as compared to their WT counterparts in all samples ($P < 0.05$; Fig. 5B–G); however, the invasion and dissemination routes were similar between the two groups.

4. Discussion

In the present study, we investigated *T. gondii* immunopathogenicity, including cytokine expression, stage conversion in gut-associated tissues, and invasion and dissemination routes after PI. Notably, we found that Th1-type cytokines—such as IFN-γ and IL-12—were highly expressed in the PP and MLN of infected WT mice, consistent with a previous report [27]. IL-10 was also induced in the PP and MLN of infected WT mice, but the Th2 cytokine IL-4 was not. IL-10 has important regulatory—mostly inhibitory—effects on immune responses [28]; however, the mechanisms regulating innate IL-10 expression following *T. gondii* infection, and the cytokine's functional role in the response to toxoplasmosis remain unclear [28]. Conversely, infected GKO mice were unable to produce adequate Th1 or Th2 cytokines, resulting in significantly decreased survival.

In nature, *T. gondii* is ingested as bradyzoites before disseminating throughout the host as tachyzoites [1]. Dubey [1] emphasized that bradyzoites retain bradyzoite-specific antigen (BAG-5) expression in the intestine even after the first division into two tachyzoites, and that all administered bradyzoites convert to tachyzoites by 18 h post-infection. Although BAG-5-positive parasites were not detected at 2–5 days after PI, this antigen reappeared at 6 days post-PI in the intestine [1]. In addition, *T.g.Hsp30/bag1* mRNA was detected in the ileum parenchyma and PP, but not in the MLN 7 days after PI in WT mice in this study. In contrast, *SAG1* mRNA was detected at much higher levels in the MLN than in the ileum parenchyma or PP. As all bradyzoites inoculated were already converted to tachyzoites [1], these results would indicate that some tachyzoites converted to bradyzoites in the ileum parenchyma and the PP, whereas this stage conversion had not yet occurred in the MLN. This may be due to a delay before the parasite reached this tissue. Thus, our data suggest that *T. gondii* undergoes bradyzoite-to-tachyzoite and tachyzoite-to-bradyzoite transformations when first invading the ileum parenchyma and PP near the site of invasion before disseminating throughout the host lymphatic system, including the MLN, as a tachyzoite. In GKO mice, *SAG1* and *T.g.Hsp30/bag1* mRNA expression was detected in all tissues analyzed, with *SAG1* mRNA expression levels considerably higher than those of *T.g.Hsp30/bag1* at 7 days after PI. As such, it appears that some *T. gondii* differentiate from the tachyzoite to bradyzoite stages even in GKO mice, with IFN-γ reportedly regulating this stage conversion [29].

There are two likely explanations for the detection of *T.g.Hsp30/bag1* mRNA in the gut-associated tissue of GKO mice. First, as *T. gondii* actively proliferated in GKO mice during acute infection, zoites may be more widely and heavily distributed, and some zoites were converted from tachyzoites to bradyzoites expressing *T.g.HSP30/bag1* mRNA. Second, stressful conditions— such as higher temperature (43 °C), altered pH (pH 6.6–6.8 or 8.0–8.2), or chemical stress (Na arsenite)—that slow growth and induce bradyzoite differentiation [30–36]— may also affect the stage conversion from tachyzoites to bradyzoites in GKO mice. After *T. gondii* infection, GKO mice developed severe diarrhea and metabolic acidosis, which may alter the pH in the ileum parenchyma, PP, and MLN, thus altering parasite proliferation. Nevertheless, further studies are needed to explain this observed phenomenon more precisely. In the PP of WT mice, *T.g.HSP30/bag1* mRNA expression levels were much higher, and *SAG1* mRNA expression levels were much lower than those in GKO mice. Thus, the stage conversion of *T. gondii* zoites from tachyzoites to bradyzoites had already begun in the PP of both WT and GKO mice and was much more prominent in the former than the latter. Detailed experimental research would be required further to determine whether cysts are formed in the ileum parenchyma or gut associated tissues.

Histology of tissues harvested 8 days after PI revealed extensive inflammatory infiltrates—including neutrophils—in the microvilli, lamina propria, PP, and MLN of WT mice. Coombes et al. [37] showed that *T. gondii* formed disconnected infection foci in the small intestine, and neutrophils and inflammatory monocytes were recruited before undergoing transepithelial migration. Neutrophils accounted for a high proportion of the infiltrate and acted as motile reservoirs for the parasite [37]. As *T. gondii* induces endothelial adhesion molecule expression and polymorphonuclear neutrophil adhesion [38], these cells may play an important role in innate immunity against this parasite in WT mice. In GKO mice, strong edema in the microvilli, lamina propria, PP, and MLN; marked necrosis and increased apoptosis in inflamed areas—particularly the PP; and significant neutrophil infiltration were the most characteristic findings. Previously, T cells in the PP were found to undergo Fas-dependent apoptosis following PI [39]; however, numerous apoptotic cells were observed in the PP of GKO mice despite undetectable *IFN*-γ mRNA expression. Programmed cell death pathways are critical to host defense mechanisms [40] and occur via three separate mechanisms: apoptosis (type I), autophagy (type II), and necroptosis (Type III) [40]. These cell-death processes are regulated by similar pathways in an IFN-γ-dependent or independent manner, indicative of complex crosstalk [41]. Thus, the numerous apoptotic cells observed in the PP of GKO mice can be explained by IFN-γ independent cell death pathways. As IFN-γ plays a key role in resistance to *T. gondii* infection, the pathologic findings observed in GKO mice are to be expected. Moreover, *T. gondii* both promotes and inhibits apoptosis [40,42,43], and although the underlying mechanisms connecting *T. gondii* infection and apoptosis have been investigated, the exact molecular basis requires further clarification.

IFN-γ is an essential effector molecule in the host defense against *T. gondii* infection [16,44]. Our investigation showed significant differences in the survival rates of WT and GKO mice after PI. Surprisingly, a ten-fold difference in *T. gondii* load was observed in the PP of WT and GKO mice by 3 days after PI. Thus, the parasite accumulates and proliferates in the PP in the early phase of invasion before disseminating through the lymphatic networks of both WT and GKO mice. An immunocompetent host cannot defend against this initial attack on the PP; however, the host can subsequently initiate an adequate Th1-type immune response, thereby preventing the growth of *T. gondii* during invasion.

Co-infection of parasites—such as *Giardia lamblia*—with enteric bacteria can affect the clinical course and disease progression [45]. In *T. gondii* infection, the involvement of the enteric bacterial flora in the pathophysiology of toxoplasmosis was recently reported [46]. Given that GKO mice are immunocompromised, it was possible that co-infection with enteric bacteria could influence the clinical course of toxoplasmosis. However, our study demonstrated that GKO mice died within 10 days of PI irrespective of treatment with antibiotics specific for enteric bacteria, suggesting that enteric bacteria have little effect on toxoplasmosis in GKO mice.

In this study, the first detected tissues and the days when the parasite DNA was detected were different in the analyses with nested PCR against the *B1* gene (35 copies [47]) and QC-PCR against the *SAG1* gene (single copy [22]). This discrepancy may be attributed to the high sensitivity of nested PCR as compared to QC-PCR. Thus, small numbers of parasites could be detected earlier using nested PCR in the ileum parenchyma rather than using QC-PCR. In addition, lymphocytes and monocytes harboring parasites may accumulate in the PP and then the parasites proliferate in the days following PI, resulting in an increased number of parasites in the PP than in the ileum parenchyma. Therefore, the number of parasites in the PP surpassed the detection threshold of both PCR methods.

The early kinetics of *T. gondii* infection after PI have been extensively investigated using tissue culture methods, histologic

examination, bioassays, QC-PCR, and real-time PCR [1,9,10,13]. There are some discrepancies in parasite dissemination, possibly because of the differences of mouse and parasite strains or infection methods employed among studies. Moreover, we reported the kinetics of parasite load in various organs [8,10,11], which also showed some discrepancies, including the results of the present study, possibly because of the differences of the numbers and sizes of cysts used, DNA purification methods, and tissue preparation protocols. In addition, the infection technique should be considered because even when using PI, inconsistent dissemination patterns were described depending on the infection method such as oral gavage or natural feeding [12].

There are two possible routes for *T. gondii* dissemination after PI [13]: direct invasion of the capillary blood vessels of the intestine followed by dissemination in hemocytes via portal blood flow, or invasion of intestinal lymphatic vessels or tissues and subsequent dissemination through the lymphatic network. Our study showed that *SAG1* genes were detected in the PP of WT mice 3 days after PI, in the ileum parenchyma and the MLN on day 5, and in the spleen, portal blood that drains intestinal blood into the general circulation, and aortic blood only on day 7, suggesting that *T. gondii* mainly accumulates and proliferates in the PP before being disseminated throughout the lymphatic system. Large numbers of lymphocytes emigrate from the PP, and reach the blood circulation after expansion and maturation within the MLN [5]. Given that intestinal lymph circulates through the thoracic duct before flowing into the superior vena cava at the angulus venosus, it is likely that parasitemia will occur at this lymph–venous interface.

5. Conclusions

Data from the present study suggest that *T. gondii* invades the ileum parenchyma during the initial stages of PI and subsequently accumulates and proliferates in the PP. These preponderances of evidence in the field now favor a model in which *Toxoplasma* follows lymphatic dissemination after PI in both immunocompetent and immunocompromised mice. Moreover, some zoites differentiate from tachyzoites to bradyzoites in the ileum. Precise studies are under investigation to analyze cyst formation in the gut.

Conflict of interest

None.

Acknowledgments

This work was supported by JSPS KAKENHI Grant Number JP20592071.

References

[1] J.P. Dubey, Bradyzoite-induced murine toxoplasmosis: stage conversion, pathogenesis, and tissue cyst formation in mice fed bradyzoites of different strains of *Toxoplasma gondii*, J. Eukaryot. Microbiol. 44 (1997) 592–602.
[2] N. Rachinel, D. Buzoni-Gatel, C. Dutta, F.J. Mennechet, S. Luangsay, L.A. Minns, M.E. Grigg, S. Tomavo, J.C. Boothroyd, L.H. Kasper, The induction of acute ileitis by a single microbial antigen of *Toxoplasma gondii*, J. Immunol. 173 (2004) 2725–2735.
[3] D. Lowe, R. Hessler, J. Lee, R. Schade, A. Chaudhary, Toxoplasma colitis in a patient with acquired immune deficiency syndrome, Gastrointest. Endosc. 63 (2006) 341–342.
[4] S.B. Cohen, E.Y. Denkers, The gut mucosal immune response to *Toxoplasma gondii*, Parasite Immunol. 37 (2015) 108–117.
[5] H.J. Rothkötter, R. Pabst, M. Bailey, Lymphocyte migration in the intestinal mucosa: entry, transit and emigration of lymphoid cells and the influence of antigen, Vet. Immunol. Immunopathol. 72 (1999) 157–165.
[6] G. Azzali, Structure, lymphatic vascularization and lymphocyte migration in mucosa-associated lymphoid tissue, Immunol. Rev. 195 (2003) 178–189.
[7] M.R. Neutra, N.J. Mantis, J.P. Kraehenbuhl, Collaboration of epithelial cells with organized mucosal lymphoid tissues, Nat. Immunol. 2 (2001) 1004–1009.
[8] K. Norose, K. Naoi, H. Fang, A. Yano, In vivo study of toxoplasmic parasitemia using interferon-γ-deficient mice: absolute cell number of leukocytes, parasite load and cell susceptibility, Parasitol. Int. 57 (2008) 447–453.
[9] M.H. Sumyuen, Y.J. Garin, F. Derouin, Early kinetics of *Toxoplasma gondii* infection in mice infected orally with cysts of an avirulent strain, J. Parasitol. 81 (1995) 327–329.
[10] W. Luo, F. Aosai, M. Ueda, K. Yamashita, K. Shimizu, S. Sekiya, A. Yano, Kinetics in parasite abundance in susceptible and resistant mice infected with an avirulent strain of *Toxoplasma gondii* by using quantitative competitive PCR, J. Parasitol. 83 (1997) 1070–1074.
[11] K. Norose, H.S. Mun, F. Aosai, M. Chen, H. Hata, Y. Tagawa, Y. Iwakura, A. Yano, Organ infectivity of *Toxoplasma gondii* in interferon-γ knockout mice, J. Parasitol. 87 (2001) 447–452.
[12] J.P. Boyle, J.P. Saeij, J.C. Boothroyd, *Toxoplasma gondii*: inconsistent dissemination patterns following oral infection in mice, Exp. Parasitol. 116 (2007) 302–305.
[13] O. Djurković-Djaković, V. Djokić, M. Vujanić, T. Zivković, B. Bobić, A. Nikolić, K. Slavić, I. Klun, V. Ivović, Kinetics of parasite burdens in blood and tissues during murine toxoplasmosis, Exp. Parasitol. 131 (2012) 372–376.
[14] C. Baliu, G. Sanclemente, M. Cardona, M.A. Castel, F. Perez-Villa, A. Moreno, C. Cervera, Toxoplasmic encephalitis associated with meningitis in a heart transplant recipient, Transpl. Infect. Dis. 16 (2014) 631–633.
[15] J.A. Fishman, Infection in solid-organ transplant recipients, N. Engl. J. Med. 357 (2007) 2601–2614.
[16] Y. Suzuki, M.A. Orellana, R.D. Schreiber, J.S. Remington, Interferon-γ: the major mediator of resistance against *Toxoplasma gondii*, Science 240 (1988) 516–518.
[17] F. Yarovinsky, Innate immunity to *Toxoplasma gondii* infection, Nat. Rev. Immunol. 14 (2014) 109–121.
[18] M.E. Grigg, J.C. Boothroyd, Rapid identification of virulent type I strains of the protozoan pathogen *Toxoplasma gondii* by PCR-restriction fragment length polymorphism analysis at the *B1* gene, J. Clin. Microbiol. 39 (2001) 398–400.
[19] K. Kamei, K. Sato, Y. Tsunematsu, A strain of mouse highly susceptible to *Toxoplasma*, J. Parasitol. 62 (1976) 714.
[20] Y. Tagawa, K. Sekikawa, Y. Iwakura, Suppression of concanavalin A-induced hepatitis in IFN-$\gamma^{-/-}$ mice, but not in TNF-$\alpha^{-/-}$ mice: role for IFN-γ in activating apoptosis of hepatocytes, J. Immunol. 159 (1997) 1418–1428.
[21] L.X. Piao, F. Aosai, M. Chen, H. Fang, H.S. Mun, K. Norose, A. Yano, A quantitative assay method of *Toxoplasma gondii* HSP70 mRNA by quantitative competitive-reverse transcriptase-PCR, Parasitol. Int. 53 (2004) 49–58.
[22] J.L. Burg, D. Perelman, L.H. Kasper, P.L. Ware, J.C. Boothroyd, Molecular analysis of the gene encoding the major surface antigen of *Toxoplasma gondii*, J. Immunol. 141 (1988) 3584–3591.
[23] W. Bohne, U. Gross, D.J. Ferguson, J. Heesemann, Cloning and characterization of a bradyzoite-specifically expressed gene (*hsp30/bag1*) of *Toxoplasma gondii*, related to genes encoding small heat-shock proteins of plants, Mol. Microbiol. 16 (1995) 1221–1230.
[24] R. Ansorg, P.M. Rath, V. Runde, D.W. Beelen, Influence of intestinal decontamination using metronidazole on the detection of methanogenic *Archaea* in bone marrow transplant recipients, Bone Marrow Transplant. 31 (2003) 117–119.
[25] M.G. Besselink, H.M. Timmerman, L.P. van Minnen, L.M. Akkermans, H.G. Gooszen, Prevention of infectious complications in surgical patients: potential role of probiotics, Dig. Surg. 22 (2005) 234–244.
[26] L. Silvestri, H.K. van Saene, D.F. Zandstra, J.C. Marshall, D. Gregori, A. Gullo, Impact of selective decontamination of the digestive tract on multiple organ dysfunction syndrome: systematic review of randomized controlled trials, Crit. Care Med. 38 (2010) 1370–1376.
[27] C.R. Sturge, F. Yarovinsky, Complex immune cell interplay in the gamma interferon response during *Toxoplasma gondii* infection, Infect. Immun. 82 (2014) 3090–3097.
[28] P.J. Gaddi, G.S. Yap, Cytokine regulation of immunopathology in toxoplasmosis, Immunol. Cell Biol. 85 (2007) 155–159.
[29] A. Yano, H.S. Mun, M. Chin, K. Norose, K. Hata, M. Kobayashi, F. Aosai, Y. Iwakura, Roles of IFN-γ on stage conversion of an obligate intracellular protozoan parasite, *Toxoplasma gondii*, Int. Rev. Immunol. 21 (2002) 405–421.
[30] M. Soête, D. Camus, J.F. Dubremetz, Experimental induction of bradyzoite-specific antigen expression and cyst formation by the RH strain of *Toxoplasma gondii* in vitro, Exp. Parasitol. 78 (1994) 361–370.
[31] M. Soête, J.F. Dubremetz, *Toxoplasma gondii*: kinetics of stage-specific protein expression during tachyzoite-bradyzoite conversion in vitro, Curr. Top. Microbiol. Immunol. 219 (1996) 75–80.
[32] L.M. Weiss, D. Laplace, P.M. Takvorian, H.B. Tanowitz, A. Cali, M. Wittner, A cell culture system for study of the development of *Toxoplasma gondii* bradyzoites, J. Eukaryot. Microbiol. 42 (1995) 150–157.
[33] L.J. Knoll, T. Tomita, L.M. Weiss, Bradyzoite development, in: L.M. Weiss, K. Kim (Eds.), Toxoplasma gondii, 2nd ed., Elsevier Ltd, 2014, pp. 521–549.
[34] M.E. Jerome, J.R. Radke, W. Bohne, D.S. Roos, M.W. White, *Toxoplasma gondii* bradyzoites form spontaneously during sporozoite-initiated development, Infect. Immun. 66 (1998) 4838–4844.
[35] W. Bohne, J. Heesemann, U. Gross, Reduced replication of *Toxoplasma gondii* is necessary for induction of bradyzoite-specific antigens: a possible role for nitric oxide in triggering stage conversion, Infect. Immun. 62 (1994) 1761–1767.
[36] L.M. Weiss, K. Kim, The development and biology of bradyzoites of *Toxoplasma gondii*, Front. Biosci. 5 (2000) D391–D405.
[37] J.L. Coombes, B.A. Charsar, S.J. Han, J. Halkias, S.W. Chan, A.A. Koshy, B. Striepen, E.A. Robey, Motile invaded neutrophils in the small intestine of *Toxoplasma gondii*-infected mice reveal a potential mechanism for parasite spread, Proc. Natl. Acad. Sci. U. S. A. 110 (2013) E1913–E1922.
[38] A. Taubert, M. Krüll, H. Zahner, C. Hermosilla, *Toxoplasma gondii* and *Neospora caninum* infections of bovine endothelial cells induce endothelial adhesion molecule gene transcription and subsequent PMN adhesion, Vet. Immunol. Immunopathol. 112 (2006) 272–283.

[39] O. Liesenfeld, J.C. Kosek, Y. Suzuki, Gamma interferon induces Fas-dependent apoptosis of Peyer's patch T cells in mice following peroral infection with *Toxoplasma gondii*, Infect. Immun. 65 (1997) 4682–4689.
[40] S.K. Halonen, Modulation of host programmed cell death pathways by the intracellular protozoan parasite, *Toxoplasma gondii* — implications for maintenance of chronic infection and potential therapeutic applications, in: T.M. Ntuli (Ed.), Cell Death–Autophagy, Apoptosis and Necrosis, InTech., 2015, pp. 373–393, , https://doi.org/10.5772/61529.
[41] V. Nikoletopoulou, M. Markaki, K. Palikaras, N. Tavernarakis, Crosstalk between apoptosis, necrosis and autophagy, Biochim. Biophys. Acta 1833 (2013) 3448–3459.
[42] C.G. Lüder, U. Gross, Apoptosis and its modulation during infection with *Toxoplasma gondii*: molecular mechanisms and role in pathogenesis, Curr. Top. Microbiol. Immunol. 289 (2005) 219–237.
[43] P.B. Nash, M.B. Purner, R.P. Leon, P. Clarke, R.C. Duke, T.J. Curiel, *Toxoplasma gondii*-infected cells are resistant to multiple inducers of apoptosis, J. Immunol. 160 (1998) 1824–1830.
[44] Y. Suzuki, Q. Sa, M. Gehman, E. Ochiai, Interferon-gamma- and perforin-mediated immune responses for resistance against *Toxoplasma gondii* in the brain, Expert Rev. Mol. Med. 13 (2011) e31.
[45] N. Muller, N. von Allmen, Recent insights into the mucosal reactions associated with *Giardia lamblia* infections, Int. J. Parasitol. 35 (2005) 1339–1347.
[46] M. Raetz, S.H. Hwang, C.L. Wilhelm, D. Kirkland, A. Benson, C.R. Sturge, J. Mirpuri, S. Vaishnava, B. Hou, A.L. Defranco, C.J. Gilpin, L.V. Hooper, F. Yarovinsky, Parasite-induced TH1 cells and intestinal dysbiosis cooperate in IFN-γ-dependent elimination of Paneth cells, Nat. Immunol. 14 (2013) 136–142.
[47] J.L. Burg, C.M. Grover, P. Pouletty, J.C. Boothroyd, Direct and sensitive detection of a pathogenic protozoan, *Toxoplasma gondii*, by polymerase chain reaction, J. Clin. Microbiol. 27 (1989) 1787–1792.